JEAS

JOURNAL OF ENGINEERING AND APPLIED SCIENCES

Journal of Engineering and Applied Sciences 9 (2013), 24-41

Finite element modelling of cassava flash drying in a vertically upward pneumatic conveying dryer

O. O. Otuu[1], Sam Omenyi[2], Solomon Nwigbo[2]

[1]*Scientific Equipment Development Institute Enugu, Enugu State, Nigeria*
[2]*Department of Mechanical Engineering, Nnamdi Azikiwe University Awka, Anambra State, Nigeria*

Abstract
A mathematical model for vertically upward pneumatic conveying drying of cassava cultivar TMe 419 was developed and solved using Finite Element approach. The work was based on two-fluid analysis and it used an iterative method to predict the gas phase variables along the flash tube while considering the influence of material on the flow stream. The gas phase variables were generated by a program coded with Comsol Script while the drying variables for a representative cassava particle were determined by finite element method implemented on Comsol Multiphysics Platform. The simulation predicted the state of the moisture along the tube under different conditions thereby providing a tool for research and design of vertical upward conveying dryers.
Keywords: cassava cultivar, flash dryer, TMe 419, finite element

1. Introduction

Moisture is responsible for the short shelf-life of most agricultural products including cassava root [1]. Therefore efforts are then geared towards removal of moisture by drying to convert the cassava roots to a more stable form and also for economic value addition to the product. Cassava root is processed into many products including cassava flour.

Flash dryers have been reported to be one of the most economical choices for drying mash and solids that have between 30 – 40% moisture content. The name flash dryer originates from the fact that drying is carried out in a short span of time usually 0.5 to 3 seconds. The principle of flash drying is to evaporate surface moisture instantaneously. Wet particulate material is entrained in hot gas or steam flowing through an insulated duct. The particles are dried and the gas or steam temperature decreases [2]. In most systems air is used as the gas. It is a well known fact that the surface area of wet lump increases as the size of lump decreases. The wet cake is disintegrated into fines to increase the surface area. The drying is instantaneous and the material remains at wet bulb temperature of air, hence it is also called as "wet bulb drying". The air velocities are similar to that of pneumatic conveying with the powder remains suspended in air and gets conveyed while drying. It is therefore called a pneumatic conveying dryer.

Current challenges for the Cassava industry in Nigeria, is the area of cassava processing in general and drying in particular, include reducing the drying time, improving throughput and product quality as well as reduction in the production cost per kg of product through appropriate equipment design.

One critical area in Flash dryer design is the solid-air interaction that occurs within the flash tube, and so there is a need to study the effect of dryer variables on drying rate so that drying rate could be optimised. Baeyens et. al. [3] pointed out that the assumption that the particle travels at a steady velocity close to the velocity of the gas phase over-predict the required dryer length by 200% to 400%.

Kuye et al, [26] used the energy balance equation as a model of the system.

$$\frac{Q}{M_s} = C_s(T_p - T_f) + X_f C_{p,l}(T_v - T_f) + (X_t - X_p)\lambda + X_p C_{p,l}(T_p - T_v) + (X_t - X_p)\, C_{p,v}(T_{v,b} - T_v)$$

The data generated by the model was used to design and fabricate a flash drier; though efficiency was improved, the data from the fabricated plant had significant variation with the model predictions. Samy et al [27] developed a model by modifying the model developed by Hamed [6] based on steady two-phase flow for drying porous materials in a vertical upward pneumatic conveyor. The governing equations for the gas and dispersed phases are derived as follows:

- The mass balance equation for the gas phase may be written as:

$$\frac{d}{dx}\left[\alpha_g \rho_g u_g A\right] = S_{mass} \quad (1)$$

-The momentum equation for the gas phase was expressed as:

$$\frac{d}{dx}\left(\alpha_g \rho_g u_g^2 A\right) = -A\frac{dP}{dx} - \alpha_g \rho_g g A - F_{wg} + S_{mom} + S_{mass} u_d \quad (2)$$

-The total energy equation for the gas phase was written as:

$$\frac{d}{dx}\left[\alpha_g \rho_g u_g A\left(H_g + \frac{u_g^2}{2}\right)\right] = Q_{wall} - \alpha_g \rho_g u_g A g + S_{mass}\left(H_{wv} + \frac{u_g^2}{2}\right) + S_{energy} \quad (3)$$

-The equation of motion of a particle in a gas was given as:

$$\frac{du_d^2}{dx} = \frac{3\rho_g C_d}{2\rho_d d_p}(u_g - u_d)|u_g - u_d| - 2g\left(1 - \frac{\rho_g}{\rho_d}\right) - f_p \frac{u_d|u_d|}{d} \quad (4)$$

-The equation for particle temperature assuming temperature is uniform throughout the particle was written as:

$$u_d m_p C_{pd} \frac{dT_d}{dx} = \chi \pi d_p^2 h(T_g - T_d) - \dot{m}_d H_{fg} \quad (5)$$

-The residence time of the particles at the gas phase was given as:

$$\frac{dt_d}{dx} = \frac{1}{u_d} \quad (6)$$

A steady- state one-dimensional model for pneumatic drying of wet particle was presented by Levy et al [7]. They assumed a two-stage drying process, with mass transfer controlled by evaporation from a saturated outer particle surface in the first stage and by diffusion within the particle in the second stage. The model predictions were compared with the experimental data obtained in large scale and pilot scale pneumatic dryers and a good agreement was obtained.

In their work, Pelegrina et al [28] presented a one-dimensional model for drying of food particles. The model took into account the particle shrinkage during the drying process and the non spherical shape of the particle was considered in drag and heat transfer coefficients. They assumed that the internal resistance does not control the mass and energy transfer between solid particles and air. They found that, in the low range of air flow rates; the pressure drop under drying conditions is higher than that under transport conditions. An opposite effect was observed at higher velocities. However, the model was not verified with experimental results.

The model proposed [28] is shown below

$$v\frac{dv}{dz} = \frac{A_p}{2V_p} C_d \frac{\rho_g}{\rho_s}(u - v)|u - v| - \left(1 - \frac{\rho_g}{\rho_s}\right) g - \frac{1}{2D_t} f_p v^2 \quad (7)$$

$$u\frac{du}{dz} = -\frac{1}{\rho_g}\frac{dP}{dz} - g - \frac{2}{D_t}u^2 f_f - \frac{A_p}{2V_p}\frac{(1-\varepsilon)}{\varepsilon} C_d (u - v)|u - v| - \frac{fS}{\rho_g}\frac{(1-\varepsilon)}{\varepsilon}(u - v) \quad (8)$$

$$\frac{dX}{dz} = \frac{1}{W_s}\frac{d}{dz}\left[\rho_s v(1-\varepsilon)A_p\right] = -\frac{Sf(1-X)}{\rho_s v} \quad (9)$$

$$\frac{dY}{dz} = \frac{1}{W_g}\frac{d}{dz}\left[\rho_g u \varepsilon A_p\right] = -\frac{Sf(1-X)}{\rho_s v}\frac{W_s}{W_g} \quad (10)$$

$$\frac{dT_s}{dz} = \frac{S}{C_{ps}\rho_s v}[Q - fH_s] \quad (11)$$

$$\frac{dT_g}{dz} = \frac{a}{C_{pg}\rho_g u}\frac{(1-\varepsilon)}{\varepsilon}(-Q) - \frac{Q_p}{W_g C_{pg}(1+Y)} - \frac{faC_{pv}}{\rho_g u C_{pg}}\frac{(1-\varepsilon)}{\varepsilon}(T_g - T_s) \quad (12)$$

Narimatsu et al [9] investigated numerically and experimentally the drying process of porous alumina and solid glass particles in a vertical dryer using the models developed in refs [10] and [28]. The model was for one dimensional incompressible flow and the internal resistance did not control the

heat and mass transfer. Dry solids were used in heat transfer experiments, and the measurements of heat transfer coefficient indicted that the maximum value of heat transfer coefficient occurred at the velocity of minimum pressure drop. Furthermore, it was noticed that the morphology of particles (porous or non porous) did not influence the air temperature profiles. The model proposed by [10] is shown below

$$\frac{d\varepsilon}{dz} = \left[\frac{g}{w(u-v)} - \frac{F_D}{w\rho_s(u-v)}\right] \quad (13)$$

$$\frac{dp}{dz} = -\left[\frac{g}{w(u-v)} - \frac{F_D}{w\rho_s(u-v)}\right]\left(\rho_s v^2 - \rho_g u^2\right) - F_f - \left[\rho_s(1-\varepsilon) + \rho_g\varepsilon\right]g \quad (14)$$

$$\frac{dv}{dz} = \frac{v}{(1-\varepsilon)}\left[\frac{g}{w(u-v)} - \frac{F_D}{w\rho_s(u-v)}\right] \quad (15)$$

$$\frac{du}{dz} = -\frac{u}{\varepsilon}\left[\frac{g}{w(u-v)} - \frac{F_D}{w\rho_s(u-v)}\right] \quad (16)$$

$$\frac{dX}{dz} = -\frac{6A_t}{W_s d_p}\frac{v(1-\varepsilon)}{u\varepsilon}k_y(Y_s - Y) \quad (17)$$

$$\frac{dY}{dz} = \frac{6A_t}{W_g d_p}\frac{v(1-\varepsilon)}{u\varepsilon}k_y(Y_s - Y) \quad (18)$$

$$\frac{dT_s}{dz} = \frac{6A_t}{W_s d_p}\frac{v(1-\varepsilon)}{u\varepsilon}\left[\frac{h(T_g - T_s) - k_y(Y_s - Y)(H_v + C_{pv}T_s)}{(C_{ps} + C_{pa}X)}\right] - \frac{C_{pa}T_s}{(C_{ps} + C_{pa}X)}\frac{dX}{dz} \quad (19)$$

$$\frac{dT_g}{dz} = \frac{6A_t}{W_g d_p}\frac{v(1-\varepsilon)}{u\varepsilon}\left[\frac{k_y(Y_s - Y)(H_v + C_{pv}T_s) - h(T_g - T_s)}{C_{pg}}\right] - \frac{C_{pv}T_g + H_v}{C_{pv}}\frac{dY}{dz} - \frac{a_t A_t U_{TC}(T_g - T\infty)}{W_g C_{pg}} \quad (20)$$

Hamed [11] presented a model for the subsonic gas particle two phase flow with the equations:
Continuity equation

$$\frac{1}{A}\frac{\partial}{\partial x}(\alpha_c \rho_c UA) = S_{mass} \quad (21)$$

Momentum equation

$$\frac{1}{A}\frac{\partial}{\partial x}(\alpha_c \rho_c U^2 A) = -\alpha_c \frac{\partial P}{\partial x} + \alpha_c \rho_c g - \frac{1}{R_h}\tau_w + S_{mass}.V + S_{mom} \quad (22)$$

Energy equation

$$\frac{1}{A}\frac{\partial}{\partial x}\left[\alpha_c \rho_c UA\left(h_c + \frac{U^2}{2}\right)\right] = -\frac{q'_w}{R_h} - \frac{1}{A}\frac{\partial}{\partial x}(Aq'_c) + \alpha_c \rho_c gU - \frac{P}{A}\frac{\partial}{\partial x}(\alpha_p VA) + S_{mass}.\left(h_s + \frac{V^2}{2}\right) + S_{energy\ p} \quad (23)$$

Aside from the work discussed so far, Kilfoil [12] developed a numerical simulation of simultaneous drying and pneumatic conveying of small metallic filter cake particles by dedicated program generated on Matlab. He used the model developed by Littman et al [13] for the evaporation of water from large glass particles in pneumatic transport. The work is relevant for estimating the coating solution feed rate and the length of the draft tube in Wurster-type particle coaters. Specifically, the rate of evaporation of water from 1 mm glass particles in a 28.45 mm tube was calculated from the model. The rate increased with solids mass flow rate, inlet air temperature and inlet particle temperature. The heat was more rapidly removed from the particle phase than from the air phase and high inlet air temperatures are tolerated. The model presupposes that the gas and particle velocities and voidage are known and that the water film on a particle is thin and uniformly distributed. Hydrodynamic considerations that impact on the calculations were discussed.

This model by Kilfoil[12] generated steady state pressure drop and required heat input during simultaneous drying and pneumatic conveying of mineral product. However the program consists of loops that contain series of equations which are evaluated sequentially with the variables changed one at a time, for each iteration. Since several variables change simultaneously in pneumatic conveying drying, the results will have limited practical application because the mechanism is that of coupled parameters changing simultaneously.

By employing a volumetric heat transfer concept, as used for rotary dryers, simple estimation procedures have been suggested [14]. These procedures assumed that the particles were travelling at a steady velocity close to the gas velocity. It was pointed out [3] that these methods can over-predict the required dryer length by 200% to 400%. This also is reasonable considering that the dominant mode of heat transfer between hot air and the dispersed medium is convective. This means that it relies mostly on difference in velocity between the hot air stream and the particle to be dried. Therefore to assume that the velocity of the particle is close to the velocity of the air for this analysis is not inadequate.

To model the acceleration zone accurately, a stepwise procedure has been suggested by many workers [15,16,1719]. Although these procedures are considerable improvements on the steady-state, Kemp et al [16], reported that they can still give

errors of 50-100% in the tube length prediction. Baeyens et al[3] and Radford [18] neglected the effect of acceleration zone near the feed point in their stepwise procedure.

A more complex model for a pneumatic dryer considering a distribution of particle sizes for steam drying of wood chips has been developed [19,20]. The model includes a comprehensive two-dimensional model for single particle drying of single wood chip and one-dimensional plug flow was assumed. The irregular movement and the non spherical shape of the wood chips were accounted for by measuring drag and heat transfer coefficients. To validate the model, measurements of the temperature and pressure profiles as well as the final moisture content were carried out, and the predictions agreed well with the experimental results. Unlike the above studies, which were performed in a vertical upward pneumatic dryer, Alvarez et al. [21] have studied numerically and experimentally the drying process in a vertical downward pneumatic dryer. The model was for non shrinkage spherical particle and steady state one-dimensional flow. Some experimental works on the pneumatic dryer were given [22, 23, 24].

Therefore there exists a need to better understand the variables that affect drying in a vertical upward pneumatic conveying drier, by modelling using Finite Element Analysis method. This is with a view to optimizing the drying of cassava mash for flour production, with the attendant savings in production cost.

The present paper determined experimentally the physical, thermal and aerodynamic properties of cassava mash, TMe 419. Developed a mathematical model and coded the model in Comsol Script to determine the gas phase variables. The solid variables were determined by Finite Element Analysis implemented on Comsol Multiphysics platform. It determined the dryer variables for air only and for dilute phase flow of material, the effect of these variables on each other and on drying rate. Understanding and predicting the variables like the air inlet velocity, temperature and pressure drop across the flash tube will assist in the selection of an appropriate blower and heat exchanger rating. It also helped to determine the optimal length of the flash tube for cassava flash drying based on mathematical model simulation and thereby provide an indispensible tool for research and the design of vertical upward pneumatic conveying drier for cassava.

2. Mathematical modelling

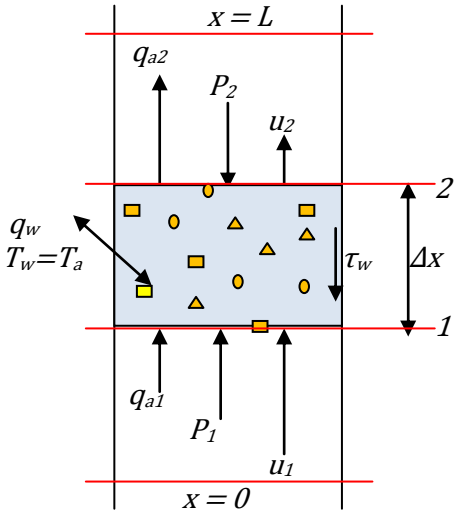


Fig. 1: Flash tube and control volume

2.1 Continuity Equation

Considering the control volume between boundaries 1 and 2 in fig. 1, the governing equations for the continuous phase (air) are derived according to the basic laws of fluid mechanics as follows:

The mass flow of the gas component (g) through the boundary (1) of the control volume per unit area is given by $\rho_g \alpha_g u_g$ and therefore the net outflow of mass of the gas component for the control volume is given by the divergence of $\rho_g \alpha_g u_g$ or

$$\frac{\partial(\rho_g \alpha_g u_g)}{\partial x} \qquad (24)$$

The rate of increase of mass of the gas component stored in the control volume is as given in equation

(24) and hence conservation of mass of the gas component demands that;
Rate of increase of stored mass (rate of accumulation) + rate of mass outflow = rate of transfer of mass from other components (rate of inflow) per unit volume

$$\frac{\partial}{\partial t}(\rho_g \alpha_g) + \frac{\partial(\rho_g \alpha_g u_g)}{\partial x} = S_{mass} \quad (25)$$

The S_{mass} term (mass transfer to the phase/unit volume) was added to the right side of the equation instead of zero (0) as in the Navier Stokes equation because there is mass transferred from the particles as drying progresses in the form of water vapour and the term accounts for it. So equation (25) is just the one dimensional Navier Stokes equation but with a mass interaction term.

$$\frac{\partial}{\partial t}(\rho_g \alpha_g) + \nabla(\rho_g \alpha_g u_g) = S_{mass} \quad (26)$$

It is important to note that Navier Stokes equation can only be used to model single phase flow situation, one component flow only and is grossly inadequate for two phase flow and hence shall not be use in this formulation.
For a duct of cross sectional area, A the continuity equation for the gas component becomes:

$$\frac{\partial}{\partial t}(\rho_g \alpha_g) + \frac{1}{A}\frac{\partial}{\partial x}(A\rho_g \alpha_g u_g) = S_{mass} \text{ (per unit volume)} \quad (27)$$

Solving the equation by considering that there is no accumulated mass in the control volume, cross sectional area is uniform and that change in density is negligible we have:

$$u_{g2} = \frac{1}{\rho_g \alpha_g} x S_{mass} + u_{g,1} \quad (28)$$

2.1.1 *Constitutive Relationships (Continuity)*

The number of particles per unit volume, N_p, can be expressed as:

$$N_p = \frac{6\alpha_s}{\pi d_p^3} \quad (29)$$

The mass transfer source term per unit length can be obtained by multiplying the evaporation rate from a single particle $\dot{m}_s$ by the number of particles in the control volume per unit length [7]

$$S_{mass} = N_p \dot{m}_s A \quad (30)$$

The mass transfer in the present model is based on a single stage drying process. In this stage, the solid surface can be considered to be fully wetted and the resistance to the mass transfer is located in the gas side. Drying starts when the particle surface receives heat from the moving air stream and evaporation commences on the surface and this is referred to as the constant-rate drying period.

At this point the transport of the water in the solid into the gas phase is driven by concentration difference and it is enhanced by convection, and it is evident that the mass flux of the water component will be higher than would occur in molecular diffusion. Convective mass transfer will occur in liquids and gases and within the structures of a porous solid. The relative contribution of molecular diffusion and convective mass transfer will depend on the magnitude of the convective currents within the gas phase. The convective mass transfer coefficient, h_m is defined as rate of mass transfer per unit area per concentration difference. Thus

$$h_m = \frac{\dot{m}_s}{A(c_{s1} - c_{s2})} \quad (31)$$

Where $\dot{m}_s$ is the mass flux (kg/s); c is concentration of the water component, mass per unit volume ((kg/m^3); A is area (m^2). The units of h_m is m/s. The coefficient represents the volume (m^3) of the water component transported across a boundary of one square meter per second

By using the relationship presented in equation (31), the mass transport due to convection becomes:

$$\dot{m}_s = \frac{h_m A M_w}{\Re T_g}(p_{s1} - p_{s2}) \quad (32)$$

The expression is used to estimate the mass flux based on the vapor pressure gradient in the region of mass transport. The humidity ratio, W (sometimes called the moisture content or the specific humidity) is defined as the mass of water vapour per unit mass of dry air and is defined by the following equation

$$W = 0.622\frac{p_{vo}}{p_{vg} - p_{vo}} \quad (33)$$

p_{vo}= partial pressure exerted by water vapor and p_{vg} = total pressure of moist air

When the specific application of mass transport is water vapour in air, Equation (33) can be incorporated into (32) to obtain:

$$\dot{m}_s = \frac{h_m A M_w P}{0.622 \Re T_A}(W_1 - W_2) \quad (34)$$

The evaporation rate from individual spherical particle submerged in a stream of drying air can be expressed as given in [46] as:

$$\dot{m}_s = h_m \chi \pi d_p^2 \left(\frac{M_w p_{vo}}{\Re T_d} - \frac{M_w p_{vg}}{\Re T_g}\right) \quad (35)$$

It is assumed that the solid particles are true spheres but with vastly increased surface area to account for the roughness and protuberances. The sphericity, χ can be defined as the ratio of the true

surface area and the spherical surface area as given in [18] as:

$$\chi = \frac{A_{so}\rho_{sa}d_p}{6} \quad (36)$$

When computing the convective transport of water vapour in air, Equations (34) or (35) can be used, and the gradient is in the form of a humidity ratio gradient in the region of convective mass transport.

For a situation that involves molecular diffusion and mass transfer due to forced convection, the following variables are important: mass diffusivity $D_{wv,g}$, from water vapour component to the gas phase, the velocity of the fluid, u_g, the density of the fluid, ρ_g, the viscosity of the fluid, μ_g, the characteristic dimension d_p, which is for our situation corresponds to the particle diameter, and the convective mass transfer coefficient h_m.

The variables are grouped into the following dimensionless numbers:

Sherwood number

$$Sh = \frac{h_m d_p}{D_{wv,g}} \quad (37)$$

Schmidt's number

$$Sc = \frac{\mu_g}{\rho D_{wv,g}} \quad (38)$$

Reynolds number

$$Re_p = \rho_g d_p |u_g - u_s|/\mu_g \quad (39)$$

Lewis number

$$L_e = \frac{h}{\rho C_p D_{wv,g}} \quad (40)$$

The functional relationship that correlated these dimensionless numbers for forced convection are:

$$Sh = f(Re_p, Sc) \quad (41)$$

The convective mass transfer coefficient for evaluating mass transfer for flow over a spherical object is obtained from an expression similar to the Froessling correlation for heat transfer as suggested in ref [45]:

$$Sh = 2.0 + \left(0.4Re_p^{\frac{1}{2}} + 0.06Re_p^{\frac{2}{3}}\right)Sc^{0.4} \quad (42)$$

After evaluating the correlation above the Sherwood number is substituted into equation (37) and h_m can then be solved for.

2.2 Momentum Equation

For the momentum balance we shall assume that the flow across the control volume is laminar and steady. The formulation for the gas momentum balance assumes for simplicity that there are no particles of the dispersed phase within the control volume. The assumption also implies that the cross-section of the particle is small and therefore the influence of the pressure gradient on the inertia of the solid particle is negligible when compared to that of the drag force. Hence the pressure gradient contributes only to the momentum of the gas.

The flux of momentum of the gas component in the k direction through the side perpendicular to the i direction is $\rho_g \alpha_g u_{gi} u_{gk}$ and hence the net flux of momentum (in the k direction) out of the control volume is given by the divergence of $\rho_g \alpha_g u_{gi} u_{gk}$ or

$$\frac{\partial(\rho_g \alpha_g u_{gi} u_{gk})}{\partial xi} \quad (43)$$

The rate of increase in momentum of gas component in the k direction

$$= \frac{\partial(\rho_g \alpha_g u_{gk})}{\partial t} \quad (44)$$

Thus the momentum conservation principle demands that the net force in the k direction acting on the gas component in the control volume (of unit volume), S_{mom} is given by:

Net rate of momentum inflow = rate of momentum accumulation + Net rate of momentum outflow

or

$$F_{gk} = \frac{\partial(\rho_g \alpha_g u_{gk})}{\partial t} + \frac{\partial(\rho_g \alpha_g u_{gi} u_{gk})}{\partial xi} \quad (45)$$

It is more difficult to construct the forces F_{gk} in order to complete the equation of motion. We must include body forces acting within the control volume:

-the force due to pressure

-the viscous stresses on the exterior of the control volume

-and most particularly, the force that each component imposes on the other component within the control volume.

The first contribution to F_{gk} is due to an external field on the gas component within the control volume, in the case of gravitational forces this is given by

$$\alpha_g \rho_g g_k \quad (46)$$

Where g_k is the component of the gravitational acceleration in the k direction (the direction of g is considered vertically downwards).

The second contribution to F_{gk} namely, that due to traction on the control volume, differ for the two phases. It is zero for the disperse phase but for the continuous phase we define a stress tensor, σ_{gki}, so that the contribution from the surface traction to the force on the phase is

$$\frac{\partial \sigma_{gki}}{\partial x_i} \quad (47)$$

σ_{gki} can be decomposed into

$$\sigma_{gki} = -P_g \delta_{ki} + \sigma^S_{gki} \quad (48)$$

Equation (47) becomes

$$\frac{\partial\left(-P_g \delta_{ki} + \sigma^S_{gki}\right)}{\partial x_i} - \frac{\partial(P_g \delta_{ki})}{\partial x_i} + \frac{\partial \sigma^S_{gki}}{\partial x_i}$$

But δ_{ki} is the Kronecker delta such that δ_{ki} = 1 for $k = i$

Therefore we have that

$$-\frac{\partial P_g}{\partial x_i}+\frac{\partial \sigma_{gki}^S}{\partial x_i} \quad (49)$$

The third contribution to F_{gk} is as a result of the force (per unit volume) imposed on the gas component by the solid component within the control volume. We write this as:

Force (imposed on gas component by solid component) = S_{mom} (50)

Now rewriting equation (45) considering the contributions of (46), (49) and (50)

$$\frac{\partial(\rho_g\alpha_g u_{gk})}{\partial t}+\frac{\partial(\rho_g\alpha_g u_{gi}u_{gk})}{\partial xi}= \alpha_g\rho_g g_k+S_{mom}-\frac{\partial P_g}{\partial x_i}+\frac{\partial \sigma_{gki}^S}{\partial x_i} \quad (51)$$

Assuming that the contribution from the surface traction to the force on the phase is negligible then equation (51) becomes

$$\frac{\partial(\rho_g\alpha_g u_{gk})}{\partial t}+\frac{\partial(\rho_g\alpha_g u_{gi}u_{gk})}{\partial xi}= \alpha_g\rho_g g_k+S_{mom}-\frac{\partial P_g}{\partial x_i} \quad (52)$$

The use of continuity equation results in the appearance of the mass interaction, S_{mass} and one obtains:

$$\rho_g\alpha_g\left\{\frac{\partial u_{gk}}{\partial t}+u_{gi}\frac{\partial u_{gk}}{\partial_{xi}}\right\}=\alpha_g\rho_g g_k+S_{mom}-S_{mass}u_{gk}-\frac{\partial P_g}{\partial x_i}+\frac{\partial \sigma_{gki}^S}{\partial x_i} \quad (53)$$

The left side of the equation is the normal rate of increase of momentum of the gas component; the term $S_{mass}u_{gk}$ is the rate of increase of the momentum in the gas component due to the gain of the mass by that phase.

For one dimensional duct flow the equation becomes

$$\frac{\partial}{\partial t}\left(\rho_g\alpha_g u_g\right)+\frac{1}{A}\frac{\partial}{\partial x}\left(A\rho_g\alpha_g u_g^2\right)=-\frac{\partial P_g}{\partial x_{ig}}-\frac{\acute{P}\tau_w}{A}+\alpha_g\rho_g g_x+S_{mom} \quad (54)$$

Where P(x) is the perimeter of the cross section and $\tau_w$is the wall shear stress.

Considering that momentum accumulation is zero for the situation being modelled, the one dimensional duct flow equation becomes:

$$\frac{1}{A}\frac{d}{dx}\left(A\rho_g\alpha_g u_g^2\right)=-\frac{dP_g}{dx}-\frac{\acute{P}\tau_w}{A}+\alpha_g\rho_g g_x+S_{mom} \quad (55)$$

Simplifying the LHS

$$\frac{d}{dx}\left(A\rho_g\alpha_g u_g^2\right)=\rho_g\alpha_g u_g^2\frac{dA}{dx}+A\alpha_g u_g^2\frac{d\rho_g}{dx}+A\rho_g u_g^2\frac{d\alpha_g}{dx}+A\rho_g\alpha_g\frac{du_g^2}{dx}$$

Applying the conditions and simplifying assumptions that were made in solving the continuity equation:

$\frac{dA}{dx}=0$, $\frac{d\alpha_g}{dx}=0$ and $\frac{d\rho_g}{dx}=0$

then equation (55) now becomes

$$\rho_g\alpha_g\frac{du_g^2}{dx}=-\frac{dP}{dx}+\alpha_g\rho_g g_x-\frac{\acute{P}\tau_w}{A}+S_{mom}$$

and

$$\frac{dP}{dx}=-\rho_g\alpha_g\frac{du_g^2}{dx}+\alpha_g\rho_g g_x-\frac{\acute{P}\tau_w}{A}+S_{mom} \quad (56)$$

but,

$$\frac{du_g^2}{dx}=2u\frac{du_g}{dx}$$

Equation (56) becomes

$$\frac{dP}{dx}=-\rho_g\alpha_g 2u_g\frac{du_g}{dx}+\alpha_g\rho_g g_x-\frac{\acute{P}\tau_w}{A}+S_{mom} \quad (57)$$

but

$\frac{du_g}{dx}=S_{mass}/\rho_g\alpha_g$

Therefore equation (57) becomes

$$\frac{dP}{dx}=-2u_g S_{mass}+\alpha_g\rho_g g_x-\frac{\acute{P}\tau_w}{A}+S_{mom}$$

Integrating we have

$$\int\frac{dP}{dx}dx=-2u_g S_{mass}\int dx+\alpha_g\rho_g g_x\int dx-\frac{\acute{P}\tau_w}{A}\int dx+S_{mom}\int dx$$

$$P=-2u_g S_{mass}x+\alpha_g\rho_g g_x x-\frac{\acute{P}\tau_w}{A}x+S_{mom}x+C \quad (58)$$

Using initial conditions

$x=0$, and $P=P_1$ then, $C=P_1$

Also $\acute{P}\tau_w=F_{wg}$ (wall shear stress per unit length) then equation (58) becomes

$$P_2=P_1-2u_g S_{mass}x+\alpha_g\rho_g g_x x-\frac{F_{wg}}{A}x+S_{mom}x \quad (59)$$

2.2.1 Constitutive Relationships (momentum)

The frictional force per unit length between the pipe wall and the gas phase was estimated by,

$$\tau_{wg}=\pi d_{pipe}\frac{f}{2}\rho_g\left(\alpha_g u_g\right)^2 \quad (60)$$

The friction factor, f, can be calculated from Blasius formulation. In addition the friction factor between particles and the wall of the pipe can be calculated as in [50]

$$f_p=1.0503Fr_p^{-1.831} \quad (61)$$

Where,

Particle Froude number,

$$Fr_p=u_s/\left(gd_p\right)^{0.5} \quad (62)$$

Equation (59) will provide the pressure at discrete points along the flash tube and this can be used to predict the flow velocity profile of the continuous phase and using the basic thermodynamic equation;

$$\frac{P_1\dot{V}_1}{T_1}=\frac{P_2\dot{V}_2}{T_2} \quad (63)$$

where, $\dot{V}$ and T are pressure, volumetric flow rate, and temperature and for a pipe section with uniform cross sectional area, we have that:

$$u_{g2}=\frac{P_1 u_{g1}T_2}{P_2T_2} \quad (64)$$

Where, $\dot{V}=Au_g$ (A = pipe cross sectional area).

This also applies to both moving bed and plug type dense phase flows. These values of air velocity are all conveying line inlet air velocity values. Air is

compressible and so as the material is conveyed along the length of a pipeline the pressure will decrease and the volumetric flow rate will increase. Thus if the pressure is one bar gauge at the material feed point in a positive pressure conveying system, with discharge to atmospheric pressure, there will be a doubling of the air flow rate, and hence velocity in a single bore pipeline. If the conveying line inlet air velocity was 20 m/s at the start of the pipeline it would be approximately 40 m/s at the outlet. The velocity, therefore, in any single bore pipeline will always be a minimum at the material feed point.

It should be emphasized that absolute values of both pressure and temperature must always be used in these equations. These velocity values are also superficial values, in that the presence of the particles is not taken into account in evaluating the velocity, even for dense phase conveying. This is universally accepted. Most data for these values, such as that for minimum conveying air velocity are generally determined experimentally or from operating experience. It is for the purposes of this work, important to take the presence of the particles into account because in accelerating the material at zero velocity at the feed point to some value along the flow line requires momentum exchange between the particles and the continuous phase.

In dilute phase conveying, with particles in suspension in the air, the mechanism of conveying is one of drag force. The velocity of the particles, therefore, will be lower than that of the conveying air. It is a difficult and complex process to measure particle velocity, and apart from research purposes, particle velocity is rarely measured. Once again it is generally only the velocity of the air that is ever referred to in pneumatic conveying.

In a horizontal pipeline the velocity of the particles will typically be about 80% of that of the air. This is usually expressed in terms of a slip ratio, defined in terms of the velocity of the particles divided by the velocity of the air transporting the particles, and in this case it would be 0.8. The value depends upon the particle size, shape and density, and so the value can vary over an extremely wide range. In vertically upward flow in a pipeline a typical value of the slip ratio will be about 0.7.
These values relate to steady flow conditions in pipelines remote from the point at which the material is fed into the pipeline, bends in the pipeline and other possible flow disturbances and shall be used as a ball pack check on the result of analytical methods. At the point at which the material is fed into the pipeline, the material will essentially have zero velocity. The material will then be accelerated by the conveying air to its slip velocity value. This process will require a pipeline length of several metres and this distance is referred to as the acceleration length. The actual distance will depend once again on particle size, shape and density.
There is a pressure drop associated with acceleration of the particles in the air stream and it has to be taken into account by some means. It is not only at the material feed point that there is an acceleration pressure drop. It is likely to occur at all bends in the pipeline. In traversing a bend the particles will generally make impact with the bend wall and so be retarded. The slip velocity at exit from a bend will be lower than that at inlet and so the particles will have to be re-accelerated back to their steady-state value. This additional element of the pressure drop is usually incorporated in the overall loss associated with a bend.
The momentum coupling source term (per unit volume) due to the reverse effect of particles can be expressed as suggested in ref [11]:

$$S_{mom} = -N_p \frac{1}{2} C_D \frac{\pi d_p^2}{4} \rho_p x\left(u_g - u_s\right)\left|u_g - u_s\right| \quad (65)$$

2.3 Energy Equation

In writing the energy equations for a multi phase flow, it is necessary to construct an energy equation for each of the phases or components. First we define a total energy density (per unit mass) e_N^* , for each component such that

$$e_N^* = e_N + \frac{1}{2} u_{Ni} u_{Ni} + gx \quad (66)$$

Then the appropriate statement of the first law of thermodynamics for each phase becomes:

Rate of heat addition to N from outside control volume, Q_N
+ Rate of work done to N by the exterior surroundings, WA_N
+ Heat transfer to N within the control volume, QI_N
+ Rate of work done to N by the other component in the control volume, WI_N
= Rate of increase of total kinetic energy of N in control volume
+ Net flux of internal energy of N out of the control volume (67)

The second term on the RHS of equation (66) contains two contributions: (i) minus the rate of work done by the stress acting on the component of N on the surface of the control volume and (ii) the rate of external shaft work, W_N, done on the component N. In evaluating the first of these, we make the same modifications to the control volume as we did for the momentum equation; specifically we make small deformations to the control volume so that its boundaries lie wholly within the continuous phase.
Then using continuous phase stress tensor,σ_{gij}, as defined earlier the expression for WA_N becomes:

$$WA_g = W_g + \frac{\partial}{\partial x_j}(u_{gi}\sigma_{gij}) \quad (68)$$

and

$$WA_s = W_N \quad (69)$$

Also the last two terms of equation (66) can be written as

$$\frac{\partial}{\partial t}(\rho_g \alpha_g e^*_{Ng}) + \frac{\partial}{\partial x_i}(\rho_g \alpha_g e^*_g u_{gi}) \quad (70)$$

Then the energy equation can be written as:

$$\frac{\partial}{\partial t}(\rho_g \alpha_g e^*_g) + \frac{\partial}{\partial x_i}(\rho_g \alpha_g e^*_g u_{gi}) = Q_g - W_g + QI_g + WI_g + \delta_g \frac{\partial}{\partial x_j}(u_{gi}\sigma_{gij}) \quad (71)$$

Note that the two terms involving internal exchange of energy between the phases may be combined into an energy interaction term given by

$$S_{energy,T} = QI_g + WI_g \quad (72)$$

It then follows that

$$\sum_N QI_g = 0$$

and

$$\sum_N WI_g = 0$$

and

$$\sum_N S_{energy,T} = 0$$

Moreover, the work done terms, WI_N, may clearly be related to the interaction forces, S_{mom}. In a two phase flow with one dispersed phase:

$$QI_g = -QI_s, \quad WI_g = -WI_s = -u_{si}F_{si}, \quad S_{energy,g} = -S_{energy,s} \quad (73)$$

When the left hand side of equation (71) are expanded and use is made of continuity equations and momentum equation , it results in the thermodynamic form of the energy equation. Using expression (71) and the relation

$$e_g = c_{Vg}T_g + constant \quad (74)$$

Between the internal energy, e_g , the specific heat capacity at constant volume, c_{Vg}, and the temperature, T_g, of the continuous phase, the energy equation can be written as

$$\rho_g \alpha_g C_{vg}\left\{\frac{\partial T_g}{\partial t} + u_g \frac{\partial T_g}{\partial x_i}\right\} = \delta_N \sigma_{gij}\frac{\partial u_{gi}}{\partial x_j} + Q_g + W_g + QI_g + S_{mom}(u_s - u_g) - \left(e^*_g - ug2Smass\right) \quad (75)$$

In equation (75) it has been assumed that the specific heat,c_{vN}, is constant and uniform. Finally the one –dimensional duct flow equation for energy balance is:

$$\frac{\partial}{\partial t}(\rho_g \alpha_g e^*_g) + \frac{1}{A}\frac{\partial}{\partial x}(A\rho_g \alpha_g e^*_g u_g) = Q_g + W_g + QI_g + WI_g + \delta_g \frac{\partial}{\partial x}(pu_g) \quad (76)$$

In simplifying the last term on the RHS of equation (75) we note that for continuous phase, $\delta_N = 1$ while for the dispersed phase, $\delta_N = 0$. And that for the flow situation under consideration, there no shaft work done on the gas component therefore we can write

$$\frac{\partial}{\partial t}(\rho_g \alpha_g e^*_g) + \frac{1}{A}\frac{\partial}{\partial x}(A\rho_g \alpha_g e^*_g u_g) = Q_g + QI_g + WI_g + \frac{\partial}{\partial x}(pu_g)$$

Since there is no energy accumulation on the control volume, this further simplifies to

$$\frac{1}{A}\frac{\partial}{\partial x}(A\rho_g \alpha_g e^*_g u_g) = Q_g + QI_g + WI_g + \frac{\partial}{\partial x}(pu_g) \quad (77)$$

now,

$$\frac{\partial}{\partial x}(A\rho_g \alpha_g e^*_g u_g) = \frac{\partial A}{\partial x}(\rho_g \alpha_g e^*_g u_g) + \frac{\partial \rho_g}{\partial x}(A\alpha_g e^*_g u_g) + \frac{\partial \alpha_g}{\partial x}(A\rho_g e^*_g u_g) + \frac{\partial e^*_g}{\partial x}(A\rho_g \alpha_g u_g) + \frac{\partial u_g}{\partial x}(A\rho_g \alpha_g e^*_g)$$

but

$$\frac{\partial A}{\partial x} = 0 \qquad \frac{\partial \rho_g}{\partial x} = 0 \quad \frac{\partial \alpha_g}{\partial x} = 0$$

So LHS of equation (77)

$$\frac{1}{A}\frac{\partial}{\partial x}(A\rho_g \alpha_g e^*_g u_g) = \frac{\partial e^*_g}{\partial x}(\rho_g \alpha_g u_g) + \frac{\partial u_g}{\partial x}(\rho_g \alpha_g e^*_g)$$

equation (77) becomes:

$$\rho_g \alpha_g \left(u_g \frac{\partial e^*_g}{\partial x} + e^*_g \frac{\partial u_g}{\partial x}\right) = Q_g + QI_g + WI_g + \frac{\partial}{\partial x}(pu_g) \quad (78)$$

$$\frac{\partial}{\partial x}(pu_g) = u_g \frac{\partial p}{\partial x} + p\frac{\partial u_g}{\partial x}$$

let

$$\frac{du_g}{dx} = S_{mass}/\rho_g \alpha_g = a$$

$$\frac{dp_g}{dx} = \alpha_g \rho_g g_x - \frac{\acute{P}\tau_w}{A} + S_{mom} - 3u_g S_{mass} = b$$

Since the values of $\frac{du_g}{dx}$ and $\frac{dp_g}{dx}$ are coefficient we replace their values with a and b for convenience

$$\frac{\partial}{\partial x}(pu_g) = (u_g b + pa)$$

Equation (78) can be rewritten as

$$\rho_g \alpha_g \left(u_g \frac{\partial e_g^*}{\partial x} + e_g^* \frac{S_{mass}}{\rho_g \alpha_g} \right) = Q_g + QI_g + WI_g + (u_g b + pa)$$

rearranging

$$\rho_g \alpha_g u_g \frac{\partial e_g^*}{\partial x} + e_g^* S_{mass} = Q_g + QI_g + WI_g + (u_g b + pa)$$

and

$$\frac{\partial e_g^*}{\partial x} + e_g^* \frac{S_{mass}}{\rho_g \alpha_g u_g} = \frac{1}{\rho_g \alpha_g u_g}\left(Q_g + QI_g + WI_g + (u_g b + pa)\right) \quad (79)$$

Again, since the entire LHS is a constant, we denote it with m for convenience

$$\frac{1}{\rho_g \alpha_g u_g}\left(Q_g + QI_g + WI_g + (u_g b + pa)\right) = m$$

Equation (78) becomes

$$\frac{\partial e_g^*}{\partial x} + e_g^* \frac{S_{mass}}{\rho_g \alpha_g u_g} = m$$

$$\frac{\partial e_g^*}{\partial x} = m - e_g^* \frac{S_{mass}}{\rho_g \alpha_g u_g}$$

$$\frac{\partial e_g^*}{\partial x} = \left(-\frac{m \rho_g \alpha_g u_g}{S_{mass}} + e_g^* \right) - \frac{S_{mass}}{\rho_g \alpha_g u_g}$$

$$\frac{\partial e_g^* / \partial_x}{e_g^* - \frac{m \rho_g \alpha_g u_g}{S_{mass}}} = -\frac{S_{mass}}{\rho_g \alpha_g u_g} \quad (80)$$

Equation (80) is variable separable and integrating we have that

$$ln\left| e_g^* - \frac{m \rho_g \alpha_g u_g}{S_{mass}} \right| = -\frac{S_{mass}}{\rho_g \alpha_g u_g} x + C$$

$$e_g^* = \left(\frac{m \rho_g \alpha_g u_g}{S_{mass}} \right) + C e^{-\frac{S_{mass}}{\rho_g \alpha_g u_g} x} \quad (81)$$

Using the following initial conditions

$$x = 0 \quad ; \qquad e_g^* = e_{g1}^*$$

Then we have

$$C = e_{g1}^* - \frac{m \rho_g \alpha_g u_g}{S_{mass}}$$

$$e_g^* = \left(\frac{m \rho_g \alpha_g u_g}{S_{mass}} \right) + \left(e_{g1}^* - \frac{m \rho_g \alpha_g u_g}{S_{mass}} \right) e^{-\frac{S_{mass}}{\rho_g \alpha_g u_g} x}$$

$$e_g^* = c_{Vg} T_g + \frac{u_g^2}{2} + gx$$

$$T_{g2} = \left(\left(\left(\frac{m \rho_g \alpha_g u_g}{S_{mass}} \right) + \left(e_{g1}^* - \frac{m \rho_g \alpha_g u_g}{S_{mass}} \right) e^{-\frac{S_{mass}}{\rho_g \alpha_g u_g} x} \right) - \frac{u_g^2}{2} - gx \right) \Big/ c_{Vg}$$

$$T_{g2} = \left(\left(\left(\frac{m \rho_g \alpha_g u_g}{S_{mass}} \right) + \left(\left(c_{Vg} T_{g1} + \frac{u_{g1}^2}{2} + gx \right) - \frac{m \rho_g \alpha_g u_g}{S_{mass}} \right) e^{-\frac{S_{mass}}{\rho_g \alpha_g u_g} x} \right) - \frac{u_g^2}{2} - gx \right) \Big/ c_{Vg} \quad (82)$$

2.3.1 Constitutive Relationships (Energy)

The energy coupling source term for the total energy equation involves convective heat transfer and the work due to particle drag as suggested in ref [11] is expressed as:

$$S_{energy} = -N_p h A \chi \pi d_p^2 (T_g - T_s) + S_{mom} u_d \quad (83)$$

The dispersed phase is introduced into the dispersing phase at a point along the flow path; the feed point which is always upstream of the flash tube. At this point the dispersed phase temperature is much smaller than the dispersing phase temperature.

Heat transfer between the phases tends to reduce the difference in temperature.

To add the component of heat transfer by convection caused by relative motion is done by defining the Nusselt number, Nu, as twice the ratio of the rate of heat transfer with convection to that

without convection. Then the rate of heat transfer becomes Nu times the above result for conduction.
The convective heat transfer coefficient, h, was calculated from Nusselt number, Nu, which is expressed as a function of Reynold number, Re_p and Prantl number, Pr, which are defined as:

$$Re = 2(u_s - u_g)R/v_g \quad (84)$$

$$Pr = \frac{\rho_g v_g C_{pg}}{k_g} \quad (85)$$

Various empirical correlations that can be used to calculate the Nusselt number has been proposed but that by Singh and Heldman [45] for a flow past a single sphere was used.

$$Nu = 2 + 0.60Re^{\frac{1}{2}}Pr^{\frac{1}{3}} \quad \text{for} \quad 1 < Re < 70000 \text{ and } 0.6 < Pr < 400 \quad (86)$$

3. Solid Phase Formulation.

Haven determined the conservation laws applicable to the continuous phase attempt shall now be made to get similar formulations for the dispersed phase. In doing this, it is important to note that, based on the dilute phase assumption, the particle is completely dispersed in the gas and so the interaction between the fluid and the dispersed particle happens on the particle scale. This means that the fluid interacts with each and every particle of the fluid and the analysis of this interaction could be described by the effect and influence of the fluid on the particle of the dispersed phase. Therefore it is important to construct the equations of motion for the individual particle. The analysis is implicitly confined to those circumstances in which the interaction between neighbouring particles are negligible.

It should also be noted that, for the situation being modelled, the dispersed phase is introduced into the dispersing phase at a point along the flow path, usually the feed point which is upstream of the flash tube. At the point of introduction the particle velocity is zero but that of the fluid is not. Drag will tend to reduce the difference. Therefore it becomes necessary to characterize the rate of equilibration of particle and fluid velocities by defining a velocity relaxation time, t_u .
It is common in dealing with gas flow laden with small particles to assume that the equation of motion can be approximated by just two terms; particle inertia and Stokes drag, which for spherical particles is [45]:

$$F_{Drag} = \frac{C_D A_p \rho_g \bar{u}^2}{2} \quad (87)$$

Where,

F_{Drag} = drag force
C_D= drag coefficient
A_p= projected particle area in the direction of motion
ρ_g= density of surrounding fluid
$\bar{u}$ = relative velocity between particle and fluid

The relative velocity decays exponentially with a time constant t_u, given by

$$t_u = m_p/6\pi R\mu c \quad (88)$$

The model assumes that the dispersed (solid) phase is moved as discrete particles and it is as discrete particles that heat is transferred to it. With that in mind, the following equations can then be written:
-The equation of motion of a particle in a gas was given as:

$$\frac{du_s^2}{dx} = \frac{3\rho_g C_D}{2\rho_s d_p}(u_g - u_s)|u_g - u_s| - 2g\left(1 - \frac{\rho_g}{\rho_s}\right) - f_p\frac{u_s|u_s|}{d_{pipe}} \quad (89)$$

$$\frac{du_s^2}{dx} = 2u_s\frac{du_s}{dx}$$

Then equation (89) can be rewritten as:

$$2u_s\frac{du_s}{dx} = \frac{3\rho_g C_D}{2\rho_s d_p}(u_g - u_s)|u_g - u_s| - 2g\left(1 - \frac{\rho_g}{\rho_s}\right) - f_p\frac{u_s|u_s|}{d_{pipe}}$$

and

$$\frac{du_s}{dx} = \frac{3\rho_g C_D}{4u_s\rho_s d_p}(u_g - u_s)|u_g - u_s| - \frac{g}{u_s}\left(1 - \frac{\rho_g}{\rho_s}\right) - f_p\frac{|u_s|}{2d_{pipe}}$$

-The equation for particle temperature assuming temperature is uniform throughout the particle was written as:

$$u_s m_p C_{ps}\frac{dT_s}{dx} = \chi\pi d_p^2 h(T_g - T_s) - \dot{m}_s H_{fg} \quad (90)$$

equation (90) can be rewritten as

$$\frac{dT_s}{dx} = \frac{\chi\pi d_p^2 h(T_g - T_s) - \dot{m}_s H_{fg}}{u_s m_p C_{ps}} \quad (91)$$

The residence time of the particle at the gas phase was calculated as:

$$-\frac{dt_s}{dx} = \frac{1}{u_s}$$

4. Cassava properties

4.1 Thermal properties:

It is obvious that the design of equipment for handling and processing cassava requires a thorough understanding of the engineering properties of cassava tuber and this is very evident for the task at hand which is the modelling of a vertical upward cassava flash dryer.

Agbetoye [26] reported the bending strength of cassava tuber while Oladele [27] reported the tensile strength, the compressive strength and elasticity of a cassava cultivar, TMS 4(2) 1425 released by IITA. Presently there are no reports in open literature on the thermal properties of the cassava cultivar, TMe 419 and these data are needed to implement mathematical models that provide insight into the drying characteristics of this material.

All of the cassava properties that are reported in this work vary with specie, maturity and moisture content and so appropriate correlations has also been developed. The intention is to generate data cassava for the purposes of design and modelling. The properties required to describe the thermal behaviour of cassava includes specific heat capacity, thermal conductivity, thermal diffusivity and heat transfer coefficient.

The determination of these properties shall relied on the empirical correlations suggested by Choi and Okos [28] which proposes that the thermal property of a food material is equal to the sum of the thermal properties of all the components of the food material. To implement these empirical correlations, proximate analysis of the food product must be carried out to determine the protein content, fat content, carbohydrate content, fibre content, ash content and moisture content. The result f the proximate analysis, the thermal properties and the thermal correlations for TMe 419 are presented by [30] and summarised below:

% Ash		1.3	(kg/kg)
% Fat		1.3	(kg/kg)
% Protein		0.59	(kg/kg)
% Moisture		60.92	(kg/kg)
% Carbohydrate	35.89	(kg/kg)	

$C_p = 3.1712 \quad \left(\frac{kJ}{kg°C}\right)$ (at 25°C and 60.92% moisture content)

$C_p = 3.1519 + 0.0006998T + 0.00000300301T^2 + 0.000000000000000008427T^3$

$C_p = 0.6264 + 0.041777\% - 0.00000000002138\%^2 + 0.00000000000002364\%^3$

$k = 0.5003 \quad \left(\frac{W}{m°C}\right)$ (at 25°C and 60.92% moisture content)

$k = 0.4617 + 0.00163T - 0.000005948T^2 + 0.000000000016484T^3$

$k = 0.07290 + 0.3557C_p - 0.1093C_p^2 + 0.01250C_p^3$

$k = 0.2559 + 0.009757\% + 0.0001497\%^2 + 0.0000009110\%^3$

$\alpha = 0.12109 \quad (\frac{m^2}{s})$ (at 25°C and 60.92% moisture content

$\alpha = 0.1119 + 0.0005761T - 0.000008321T^2 - 0.0000000000006345T^3$

$\alpha = 0.03602 + 0.001396\% + 0.000000001150\%^2 - 0.000000000007489\%^3$

$\alpha = 0.01508 + 0.03343C_p + 0.0000008521C_p^2 - 0.0000001.02741C_p^3$

$\alpha = -0.6531 + 5.4373k - 14.4307k^2 + 13.3006k^3$

4.2 Cassava properties: Physical and Aerodynamic

Understanding the variables and their effect on the performance of pneumatic conveying drying equipment is very essential in the design and modelling of pneumatic conveying systems and dryers. Variables like the particle shape, particle hardness and friability, others includes minimum carrying velocity, terminal velocity, drag force, pipe conveying capability, air velocity profile along the flash tube (with and without material flow), pressure drop along the flash tube (with and without material flow). These data will help designers in selecting an optimal pipe diameter for a conveying-drying duty, and also selection of appropriate blower and heat exchanger required to perform the heating duty.

The physical and aerodynamic properties of grated and dewatered cassava cultivar, TMe 419 was determined by [101] in order to provide information for design and adjustment of machines that require some sort of pneumatic conveyance. In his work Otuu and Omenyi [101] determined experimentally, the properties of the cassava cultivar such as particle shape, particle density, particle size, particle hardness, friability, terminal velocity and drag coefficient. The cassava particle was found to have a true density of 1083.53kg/m^3 and of very irregular shape. The size distribution and mean particle size for cassava size-reduced on a grater was found to be unique to the grater. The particle hardness for the cultivar was found to be 0.769kg/mm^2 indicating that the erosiveness of cassava particle in pneumatic conveyance is insignificant. The experimental and theoretical terminal velocities for particles of different sizes was determined and a third order regression was used to generate a correlation that predicted the terminal velocity for a given particle size of the range between 0.155mm to 6.350mm in diameter. It was also discovered that for all particle sizes, the theoretical terminal velocities was more than the experimental terminal velocities due to the rotation of the particles as they are conveyed. The result of the aerodynamic properties of cassava mash are summarised below:

Table 1: Terminal Velocities

Opening Size (mm)	Geometric mean diameter, d_g (m)	Dia. Of equivalent sphere, d_e (mm)	Sphericity, ϕ	Particle shape factor, Z	Theoritical terminal velocity, V_{tt} (m/s)	Experimental terminal velocity V_{et} (m/s)
6.350	6.350	6.658	0.819	0.494	12.954	13.38
5.027	5.027	3.803	0.807	0.183	5.958	8.92
1.438	1.438	1.463	0.495	0.273	4.508	4.61
1.226	1.226	0.986	0.440	0.120	2.452	3.20
0.874	0.874	0.642	0.665	0.138	2.124	2.40
0.582	0.582	0.420	0.509	0.100	1.461	2.00
0.150	-	-	-	-	-	-

5. Solution method

The gas phase equations were solved together with the constituitive relations using a single step iterative method to predict variables at each discrete point along the length of the tube. The entire gas phase domain was broken into cells and the condition of flow at the entrance of the cell was specified and used to determine the value of the variables at the exit. The exit values for the first cell now became the inlet values for the adjacent cell and the average value of the variables between the inlet and the outlet are used to calculate the solid phase state using Fourth Order Runge Kutta. The entire gas phase scheme was coded and implemented using Comsol Script and the program repeats the calculation until the tube length is reached or expected moisture content is attained. The diffusion of heat towards the particle centre and moisture out of the particle into the gas stream is determined by Finite Element Analysis implemented on Comsol multiphysics Platform.

6. FEA modelling

Haven determined through the Comsol Script program the condition of the air stream as it interacts with the particle along the tube length. It is necessary to determine, by the use of Finite Element Analysis method, what happens within the cassava particle under these external conditions especially to moisture content.

6.1 FEA modelling equations

The fundamental law governing all heat transfer is the first law of thermodynamics, commonly referred to as the principle of conservation of energy. However, internal energy, *U*, is a rather inconvenient quantity to measure and use in simulations. Therefore, the basic law is usually rewritten in terms of temperature, *T*. For a fluid, the resulting *heat equation* is:

$$\rho C_p\left(\frac{\partial T}{\partial t}+(u\cdot\nabla)T\right)=-(\nabla\cdot q)+\tau:S-\frac{T}{\rho}\frac{\partial p}{\partial T}\Big|_p\left(\frac{\partial p}{\partial t}+(u\cdot\nabla)p\right)+Q \quad (92)$$

where

- ρ is the density (kg/m^3)
- C_p is the specific heat capacity at constant pressure (J/(kg·K))
- T is absolute temperature (K)
- $\mathbf{u}$ is the velocity vector (m/s)
- $\mathbf{q}$ is the heat flux by conduction (W/m^2)
- p is pressure (Pa)
- τ is the viscous stress tensor (Pa)
- $\mathbf{S}$ is the strain rate tensor (1/s): $S=\frac{1}{2}(\nabla u+(\nabla u)^T)$
- Q contains heat sources other than viscous heating (W/m^3)

In deriving equation (92), a number of thermodynamic relations have been used. The equation also assumes that mass is always conserved, which means that density and velocity must be related through:

$$\frac{\partial\rho}{\partial t}+\nabla\cdot(\rho v)=0$$

The Fourier's law of conduction which states that the conductive heat flux, $\mathbf{q}$, is proportional to the temperature gradient:

$$q_i=-k\frac{\partial T}{\partial x_i} \quad (93)$$

where k is the thermal conductivity (W/(m·K)). In a solid, the thermal conductivity can be different in different directions. Then k becomes a tensor

$$k = \begin{bmatrix} k_{xx} & k_{xy} & k_{xz} \\ k_{yx} & k_{yy} & k_{yz} \\ k_{zx} & k_{zy} & k_{zz} \end{bmatrix}$$

and the conductive heat flux is given by

$$q_i = -\sum_j k_{ij} \frac{\partial T}{\partial x_j}$$

The second term on the right of equation (92) represents viscous heating of a fluid. An analogous term arises from the internal viscous damping of a solid. The operation ":" is a contraction and can in this case be written on the following form:

$$a : b = \sum_n \sum_m a_{nm} b_{nm} \qquad (94)$$

The third term represents pressure work and is responsible for the heating of a fluid under adiabatic compression and for some thermo-acoustic effects. It is generally small for low Mach number flows. A similar term can be included to account for thermo-elastic effects in solids.

Inserting equation (93) into equation (92), reordering the terms and ignoring viscous heating and pressure work puts the heat equation on a perhaps more familiar form:

$$\rho C_p \frac{\partial T}{\partial t} + \nabla \cdot (-k \nabla T) = Q - \rho C_p u \cdot \nabla T \qquad (95)$$

The General Heat Transfer application mode of Comsol Multiphysics solves this equation for the temperature, *T*.

This work determined that the specific heat capacity varies with temperature according to the expression:

$C_p = 3.1519 + 0.0006998T + 0.00000300301T^2 + 0.000000000000000008427T^3$ (J/kg.K)

where $\Delta T = (T - 0\ °C)$ and the dimensions of the numerical coefficients are such that the dimension of C_p is as stated.

For the moisture concentration, apply the diffusion equation

$$\frac{\partial c}{\partial t} + \nabla . (-D \nabla c) = 0$$

where *c* is the moisture concentration (kg/m^3), and *D* is the diffusion coefficient (m^2/s).

6.2 Model Geometry/ Solution Domain

The figure below depicts a particle of TMe 419 undergoing pneumatic conveying drying. The particle geometry is represented by an equivalent sphere as determined earlier. In applying symmetry as a modelling technique, it is easy to see that the 3 dimensional model could indeed be modelled as a 2 dimensional axisymmetric model (2d quadrant) while capturing all the details of the sphere thus simplifying the modelling effort and reducing simulation time considerably. Consequently this particle shall be modelled as a two dimensional quadrant as shown below.

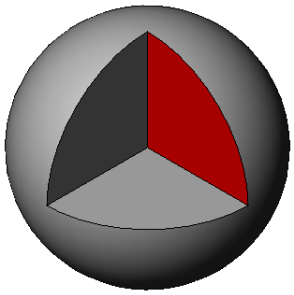


Fig. 2: Model geometry of TMe 419 particle

The model geometry is replicated in comsol multiphysics platform and is as shown below:



Fig 3: Geometric model of cassava Particle

6.3 Boundary numbering and boundary conditions:

These simplifications result in a simple domain with diameter of 5.027mm and a radius of 2.5135mm (or radius of equivalent sphere). The figure below describes the boundary numbering used when specifying the boundary conditions.

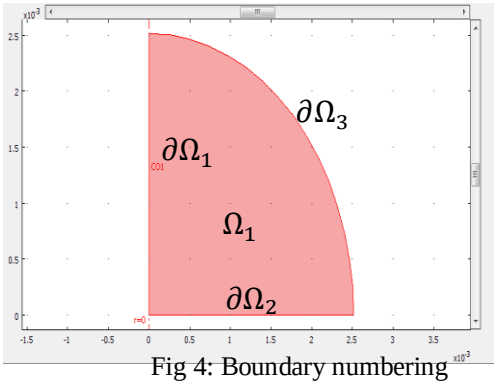


Fig 4: Boundary numbering

The heat equation accepts two basic types of boundary conditions: specified temperature and specified heat flux. The former is of Dirichlet type and prescribes the temperature at a boundary:
$T = T_0$ on $\partial\Omega$

while the latter specifies the inward heat flux
$-n \cdot \boldsymbol{q} = q_0$ on $\partial\Omega$

where:
· $\boldsymbol{q}$ is the total heat flux vector (W/m^2)

$$\boldsymbol{q} = -k\nabla T + \rho C_p \boldsymbol{u} T$$

· n is the normal vector of the boundary
· q_0 is the inward heat flux (W/m^2)

However, when convective heat transfer is active, heat flux boundary condition is a mixed, or Robin type boundary condition rather than a pure Neumann boundary condition

The special case $q_0 = 0$ is called *thermal insulation.* Another special case is $q_0 = \rho C_p \boldsymbol{u} T$, or equivalently $-n \cdot (-k\nabla T)$, which is known as convective flux. This is usually the appropriate condition on an outflow boundary in a model with convection. If the velocities are zero, thermal insulation and convective flux are equivalent conditions.
The inward heat flux q_0 is normally a sum of contributions from different heat transfer processes. It is often convenient to split the heat flux boundary condition as

$$-\boldsymbol{n} \cdot \boldsymbol{q} = q_0 + q_r + q_s + h(T_{inf} - T) \text{ on } \partial\Omega$$

where q_r represents incoming radiation and q_s is a contribution from a thin but highly conducting shell in contact with the boundary. The last term is a product of a heat transfer coefficient, h, and the difference between the surface temperature T and a reference temperature T_{inf}. It can be used to model a thin shell with low thermal conductivity or, more commonly, the convective cooling of a surface exposed to a flowing fluid with bulk temperature T_{inf}.

The equations describing moisture diffusion are coupled to the heat equation in the following two ways:

The thermal conductivity, k, increases with moisture concentration according to
k =(0.2559+0.0098[kg/mol]*c/rho)[W/(m*K)]

Where concentration, c, and the density, ρ, must be expressed in the previously stated units.
The vaporization of water at the cassava particle outer boundaries generates a heat flux out of the particle. This heat flux is represented with the term $D_m \lambda \nabla c$ in the boundary condition for boundary 3.

Where D_m is the moisture diffusion coefficient (m^2/s) from the particle to the surrounding air and λ is the latent heat of vaporisation (J/kg)

Assume symmetry for the temperature field on Boundaries 1 and 2. Air convection adds heat on Boundaries 3 and 4. According to the assumptions made earlier, add a term for the heat flux out of the cassava particle due to moisture vaporization on Boundaries 3 and 4.
Summarizing, the boundary conditions for the general heat transfer application mode are:
$\boldsymbol{n} \cdot (-k\nabla T) = 0$ at $\partial\Omega_1$ and $\partial\Omega_2$
$\boldsymbol{n} \cdot (k\nabla T) = h_T(T_{inf} - T) + \boldsymbol{n} \cdot (D_m \lambda \nabla c)$ at $\partial\Omega_3$
Where h_T is the heat transfer coefficient (W/(m^2.K)), and T_{inf} is the conveying aoir temperature.
The boundary conditions for the diffusion application mode are
$\boldsymbol{n} \cdot (-D\nabla \mathrm{c}) = 0$ at $\partial\Omega_1$ and $\partial\Omega_2$
$\boldsymbol{n} \cdot (D\nabla \mathrm{c}) = k_c(c_b - c)$ at $\partial\Omega_3$

where D is the moisture diffusion coefficient in the cassava particle (m^2/s), k_c refers to the mass transfer coefficient (m/s), and c_b denotes the outside air (bulk) moisture concentration (kg/m^3).

The diffusion coefficient and the mass transfer coefficient are given, respectively, by

$$D = \frac{k_m}{\rho C_m}, \quad k_c = \frac{h_m}{\rho C_m}$$

where C_m equals the specific moisture capacity (kg moisture/kg meat), k_m refers to the moisture conductivity (kg/(m·s)), and h_m denotes the mass transfer coefficient in mass units (kg/(m^2·s)).

7. Results/Discussion

The most interesting result from this simulation is the time required to heat the cassava particle from ambient to above 110 °C is within the 3s limit for flash drying. The section at the middle of the patty (at the lower left corner of the modeling domain) takes the longest time to reach this temperature. Figure 5 illustrates the resulting temperature field after 840 s. The temperature at the lower left corner is 70 °C, and the temperature rises toward the outside boundaries.

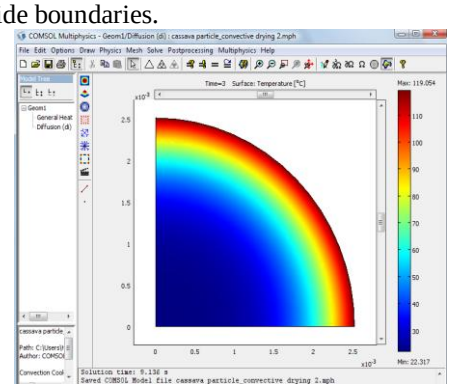


Figure 5: Temperature field after 3s at gas phase temperature of 160 °C.

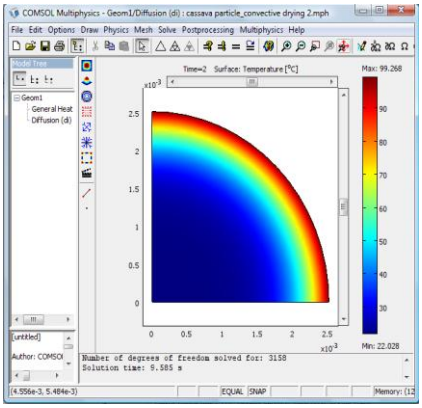


Figure 6: Temperature field after 2s at gas phase temperature of 160 °C.

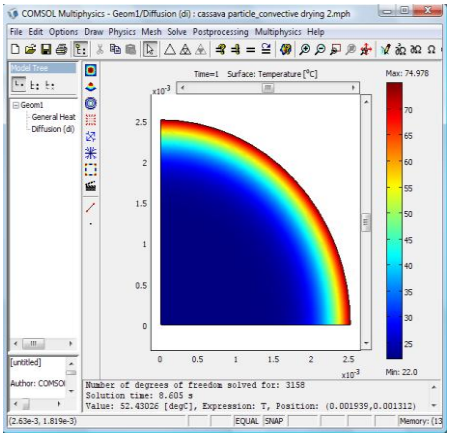


Figure 7: Temperature field after 1s at gas phase temperature of 160 °C.

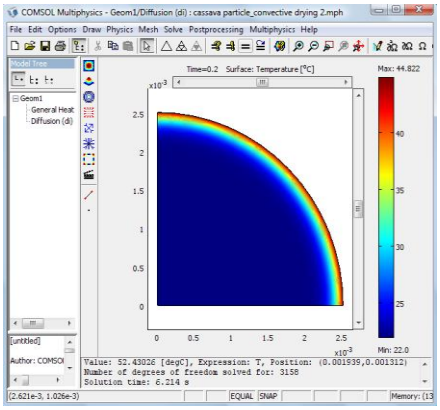


Figure 8: Temperature field after 0.2s at gas phase temperature of 160 °C.

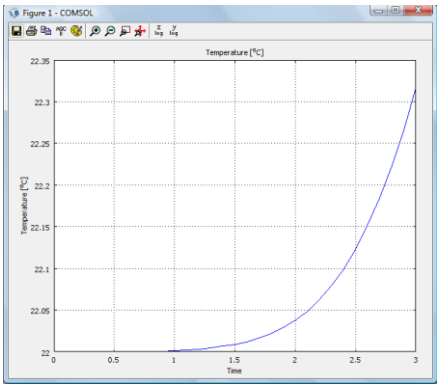


Figure 9: Temperature increase over 3s in the middle of the particle (temperature=160 °C).

8. Conclusion

The simulation revealed the state of the particle at different residence time (0.2-3s) and the particle surface temperature was found to increase as residence time increased. Similarly under the moisture content was found to reduce with increasing residence time. Finally the prediction of the tube length is derived simply from the residence time that produced the acceptable final moisture content. The other flow parameters especially those relating to the gas phase were generated from the comsol script program.

References

[1] http://www.fiiro-ng.org/cassava-flour.htm, accessed 18/06/10

[2] Saastamoinen, J. (1992), *Model of flash drying*, Proceedings of the 8th International Drying Symposium (IDS'92), Montreal, Quebec, Canada, August 2-5, pp434 – 443

[3] Baeyens J., Gauwbergen D. V. and Vinckier I., 1995, "Pneumatic Drying: the Use of Large-Scale Data in a Design Procedure", PowderTech., Vol. 83, pp. 139-148.

[26] Ayo Kuye O., Lateef Sanni, Gbassey Tarawali, Ayo D. B,Raji A.O., Otuu Obinna O., Kwaya E.I, Kareem Babatunde, Asiru Bolanle, 2009, " Conceptual Design of Cassava Flash Drier", Technical Report.

[27] Samy M. El-Behery, W.A. El-Askary, K.A. Ibrahim and Mofreh H. Ahmed, 2009,"Porous Particle Drying in a Vertical Upward Pneumatic Conveying Dryer", World Academy of Science, Engineering and Technology, Vol 53.

[6] Hamed M. H., 2005," Choked Gas-Solid Two-Phase Flow in Pipes", J.Eng. Applied Science, Faculty of Engineering, Cairo University, Vol. 52, pp. 961-980.

[7] Levy A. and Borde I., 1999, "Steady State One Dimensional Flow Model for a Pneumatic Dryer", Chem. Eng. Processing, Vol. 38, pp. 121-130.

[28] Pelegrina A. H. and Crapiste G. H., 2001, "Modelling the Pneumatic Drying of Food Particles", J. Food Eng., Vol. 48, pp. 301-310.

[9] Narimatsu C. P., Ferreira M. C. and Feire J. T., 2007, "Drying of Coarse Particles in a Vertical Pneumatic Conveyor", Drying Tech., Vol. 25, pp. 291-302.

[10] Rocha, S.C.S. (1988), Contribution to study of vertical pneumatic drying: simulation and influence of the gas-solid heat transfer coefficient, PhD Thesis (in Portuguese), Escola Politécnica/USP, São Paulo, SP, 258 p.

[11] Hamed M. H., 2005," Choked Gas-Solid Two-Phase Flow in Pipes", J. Eng. Applied Science, Faculty of Engineering, Cairo University, Vol. 52, pp. 961-980.

[12] Kilfoil M., 2003, "Numerical Simulation of Simultaneous Drying and Pneumatic Conveying: Small Metallic Filter Cake Particles", South African Institute of Mining and Metallurgy.

[13] Littman, H., Day, J-Y and Morgan M.H., 2000, "A Model for the Evaporation of Water from Large Glass Particles in Pneumatic Transport", *The Canadian Journal of Chemical Engineering*, vol. 78, part 1, Feb. 2000, pp. 124–131.

[14] Moyers C.G and Baldwin G.W., 1997, "Psychrometery, Evaporative Cooling, and Solid Drying,"Perry's Chemical Engineer's Handbook, 7th Ed., McGraw-Hill, Inc.

[15] Thorpe G.R., Wint A. and Coggan G.C., 1973, "The Mathematical Modelling of Industrial Pneumatic Driers", Transactions of the Institution of Chemical Engineers, Vol. 51, pp. 339–348.

[16] Kemp I. C., Bahu R. E. and Pasley H. S., 1994, "Model Development and Experimental Studies of Vertical Pneumatic Conveying Dryers", Drying Tech., Vol. 12, pp. 1323-1340.

[17] Kemp I. C and Oakley D. E., 1997, "Simulation and Scale-up of Pneumatic Conveying and Cascading Rotary Dryers", Drying Tech., Vol. 15, pp. 1699-1710.

[18] Radford R. D., 1997, "A Model of Particulate Drying in Pneumatic Conveying Systems", Powder Tech., Vol. 93, pp. 109-126.

[19] Fyhr C. and Rasmuson A., 1997, "Mathematical Model of Pneumatic Conveying Dryer", AICHE Journal, Vol. 43, pp. 2889-2902.

[20] Fyhr C. and Rasmuson A., 1997, "Steam Drying of Wood Ships in Pneumatic Conveying Dryers", Drying Tech., Vol. 15, pp. 1775-1785.

[21] Alvarez P. I., Vega R. and Blasco R., 2005, "Cocurrent Downflow Fluidized Bed Dryer: Experimental Equipment and Modeling", Drying Tech., Vol. 23, pp. 1435-1449.

[22] NamKung W. and Cho M., 2004, "Pneumatic Drying of Iron Ore particles in a Vertical tube", Drying Tech., Vol. 22, pp. 877-891.

[23] Kaensup W., Kulwong S. and Wongwises S., 2006, "A Small-Scale Pneumatic Conveying Dryer of Rough Rice", Drying Tech., Vol. 24, pp. 105-113.

[24] Kaensup W., Kulwong S. and Wongwises S., 2006, "Comparison of Drying Kinetics of Paddy Using a Pneumatic Dryer with and without a Cyclone", Drying Tech., Vol. 24, pp. 1039-1045.

[25] Rodolfo R. Rosales, Adam Powell, Franz-Josef Ulm, Kenneth Beers, 2006,"Continuum Modelling Simulation", MIT.

[26]Agbetoye, L.A.S (1999). The Bending Strength of Cassava Tuber, Journal of Science, Engineering and Technology, 6(2) 1800-1808

[27]Oladele P. K, Leo Ayodeji A, A. S. Ogunlowo, (2007), 'Strength and Elastic Properties of Cassava Tuber'. International Journal of Food Engineering, Volume 3, issue 2.

[28] Choi Y. and Okos M. R. (1986). "Effect of temperature and composition on the thermal properties of food". In "Food Engineering and Process Applications,"Vol 1, pp 93-101. Elsevier Applied Science Publishers, London.

[29] Otuu O. O and Omenyi S. O.(2012). "Physical and Aerodynamic Properties of Cassava Mash" unpublished paper.

[30] Otuu O. O and Omenyi S. O.(2012). "Experimental determination of Cassava Thermal Properties." unpublished paper.